Supporting Information

Modulate Hybrid Organic–Perovskite Photovoltaic Performance by Controlling the Excited Dynamics of Fullerenes

Chang-Zhi Li, [a] Po-Wei Liang, [a] Dana B. Sulas, [b] Phu D. Nguyen, [b] Xiaosong Li, [b] David S. Ginger, [b] Cody W. Schlenker, [b] and Alex K.-Y. Jen [a, b,*]

[a]Department of Materials Science and Engineering, University of Washington, Seattle, WA 98195, USA.

[b]Department Chemistry, University of Washington, Seattle, WA 98195, USA

E-mail: ajen@u.washington.edu

Table of Contents

General. All reactions dealing with air- or moisture-sensitive compounds were carried out using standard Schlenk technique. All ^{1}H (500 MHz) and ^{13}C (125 MHz) spectra were recorded on Bruker AV500 spectrometers. Spectra were reported in parts per million from internal tetramethylsilane (δ 0.00 ppm) or residual protons of the deuterated solvent for ^{1}H NMR and from solvent carbon (e.g. δ 77.00 ppm for chloroform) for ^{13}C NMR. Cyclic voltammetry (CV) measurements were carried out in a one-compartment cell under N_2, equipped with a glassy-carbon working electrode, a platinum wire counter electrode, and an Ag/Ag+ reference electrode. Measurements were performed in dichloromethane solution (0.5 mM) containing Tetrabutylammonium Hexafluorophosphate (0.1 M) as a supporting electrolyte with a scan rate of 100 mV/s. The $E_{Fc/Fc+}$ is measured to be 515 mV. P-tosylhydrazides and TPA-fullerenes were synthesized according to literature methods.[1, 2] [60]fullerene was purchased from American Dye Source. Unless otherwise noted, materials were purchased from Aldrich Inc., and used after appropriate purification.
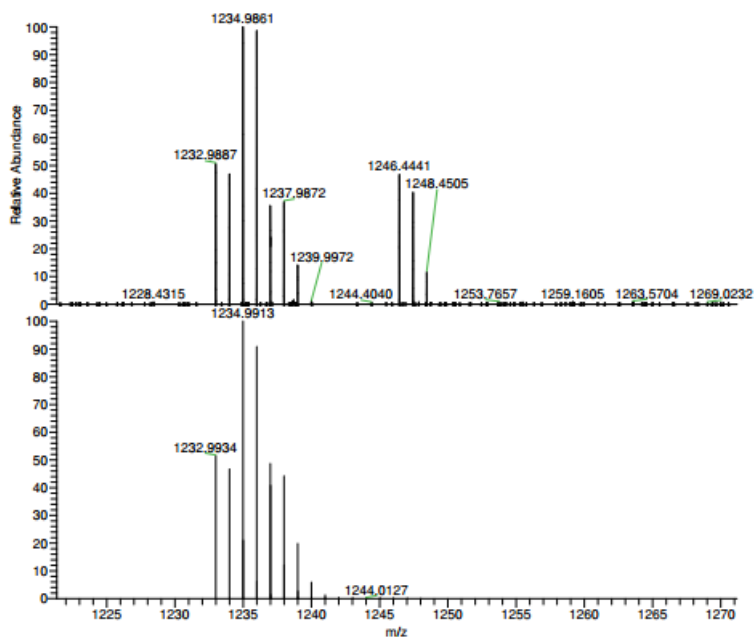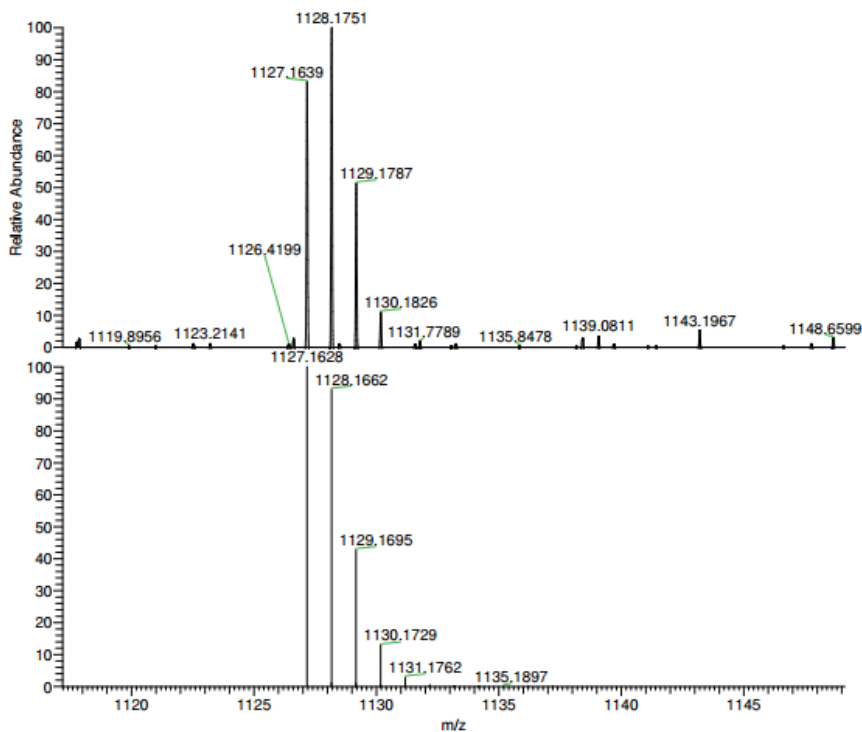
1. Synthetic Scheme for Functional TPA-PC$_{61}$BM and Chemical structure for Bis-C60 ETL
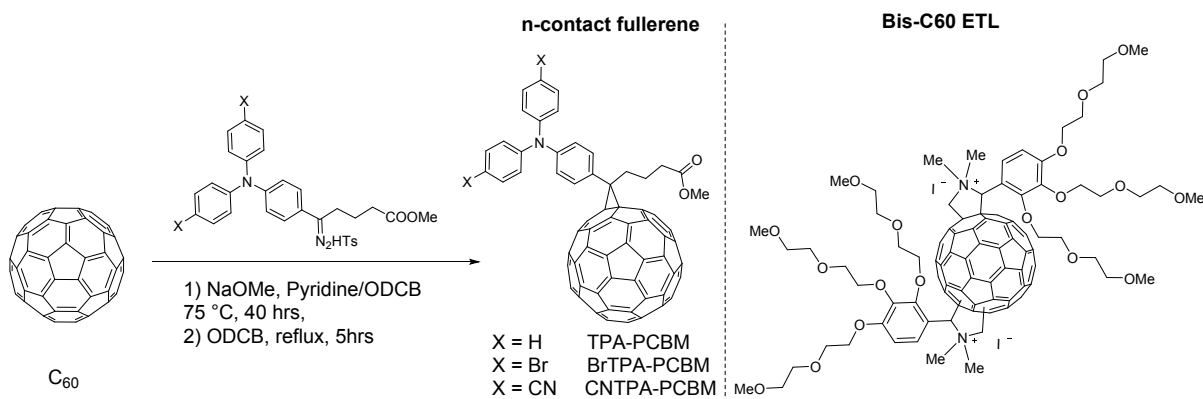
2. Electrospray Ionization Mass Spectrometry analysis

Figure S1. Electrospray Ionization Mass Spectrometry analysis and isotopic simulation were used to confirm for BrTPA-PCBM formula of $C_{84}H_{21}Br_2NO_2$.

**Figure S2**. Electrospray Ionization Mass Spectrometry analysis and isotopic simulation were used to confirm for CNTPA-PCBM formula of $C_{86}H_{21}N_3O_2$.

3. Photoinduced Absorption and Photoluminescence Measurements

Near-steady-state photoinduced absorption and photoluminescence spectra were simultaneously recorded on a home-built spectrometer using standard lock-in techniques. Excitation with a 447 nm LED (Luxeon Rebel, 700mW, LXML-PR01-0425) pump was modulated at 200 Hz by an Aligent 33120A arbitrary waveform generator, and probe light was detected using an Acton monochromator and Si/InGaAsdual-band photodiode (ThorLabs, DSD2). Photoluminescence signal was detected by blocking probe light with a home-built shutter. The signal was amplified with a Stanford Research Systems SR570 low-noise current preamplifier and measured on a Stanford Research Systems SR830 lock-in amplifier. Spectra were corrected for lamp intensity and detector response by recording total transmission intensity with a Kiethey 2000 sourcemeter. The lock-in phase was set using reflected pump light such that the signal was entirely in the positive X-channel (in-phase). Photoluminescence spectra were corrected for detector response using a calibrated LS-1-CAL ocean optics light source. Samples were held under active 20 mTorr vacuum during the measurement.
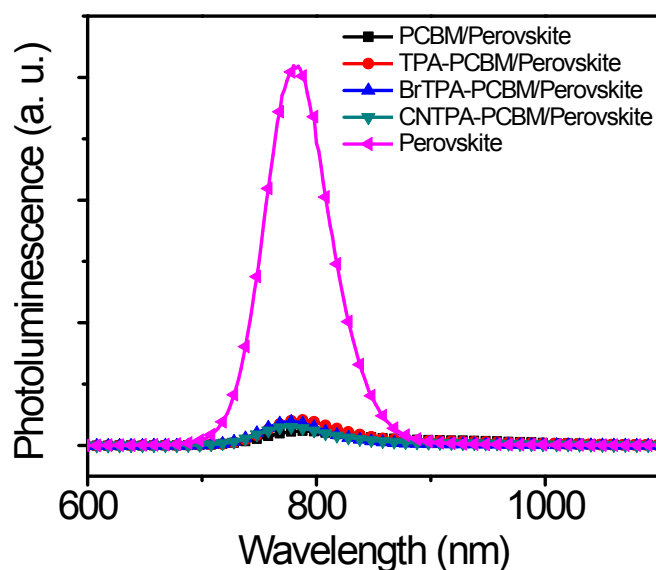
Figure S3. Photoluminescence spectra of Glass/Perovskite film and Glass/Perovskite/Fullerene film.

4. Perovskite PV Characterization
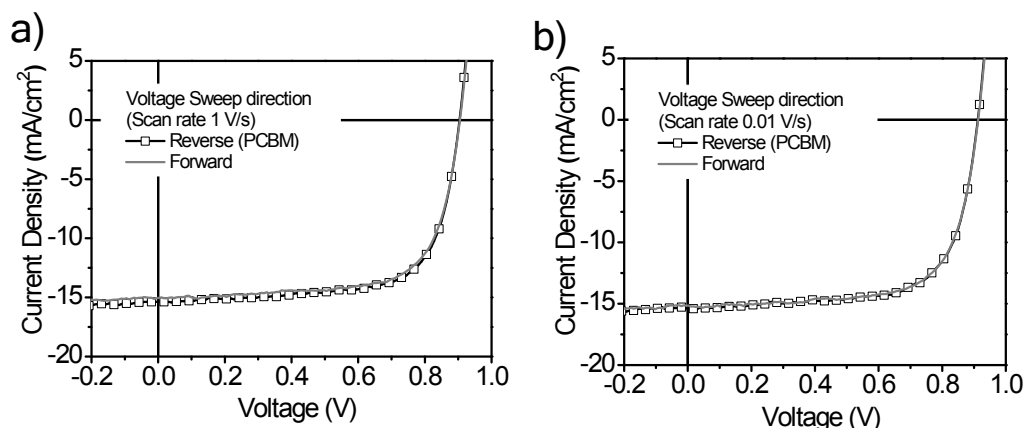
Figure S4. Current density−voltage curves by reverse and forward sweeping at the different rate of (a) 1 V/s and (b) 0.01 V/s demonstrates the absence of hysteresis in device configuration of ITO/PEDOT:PSS/$CH_3NH_3PbI_{3-x}Cl_x$/PCBM/Bis-C_{60}/Ag devices. Similar trend are observed from PHJ devices using TPA-PCBM, BrTPA-PCBM and CNTPA-PCBM.

5. Details of Computational Modeling

All calculations were performed in the Density Functional Theory (DFT) framework as implemented in the development version of the GAUSSIAN software suite[3]. We obtained the ground state geometries, energies, dipoles and electronic structures of the four fullerenes by solving the Kohn-Sham equations self-consistently using the B3LYP exchange correlation functional and 6-31G(d) basis set.[4,5,6] The same ground state calculations had been repeated just for TPA-PCBM using the cc-pvdz and cc-pvtz basis sets, yielding negligible differences compared to the results using 6-31G(d) so the smaller basis set was chosen for the sake of computational efficiency. We used Mulliken population analysis to characterize and visualize the frontier MOs, i.e. HOMO and LUMO, thus identified TPA-PCBM and BrTPA-PCBM as the fullerenes with charge transfer due to the physical separation of the HOMO and LUMO. To confirm that the excitation from HOMO to LUMO is indeed an allowed transition, we used linear response TD-DFT where excited states are generated by vertical excitation between molecular orbitals based on the transition dipole moments. For all four fullerenes,

the HOMO to LUMO excitation was found to dominate the first singlet excited state. The charge separation of the electron-hole from this first excited state was visualized by plotting the difference between excited state's and ground state's charge densities.
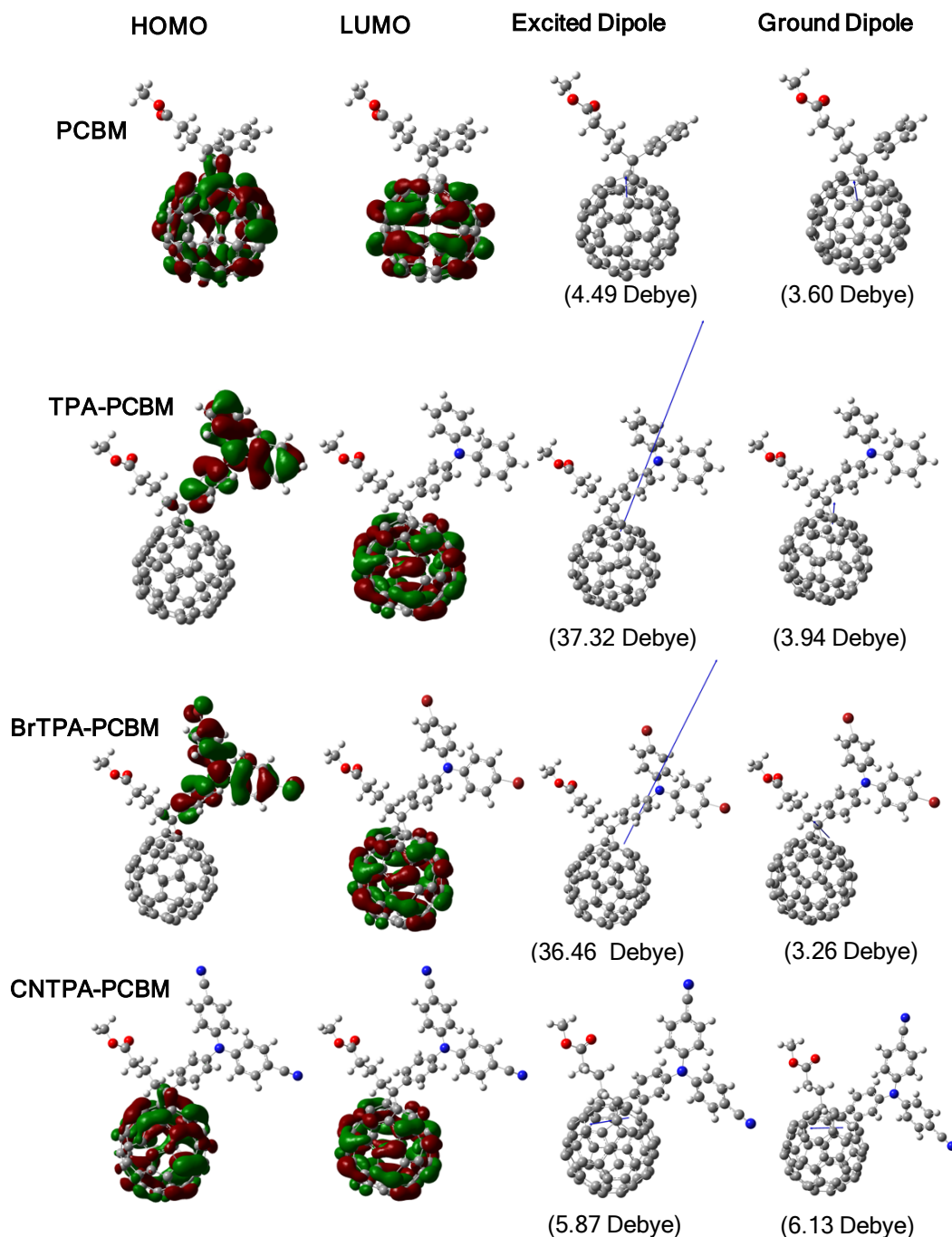
Figure S5. Electron density distribution of the frontier molecular orbitals (LUMO and HOMO), neat excited and ground dipole for PCBM, TPA-PCBM, BrTPA-PCBM and CNTPA-PCBM.

6. OFET and SCLC Characterization

***Device Fabrication and Characterization of FET*:** Field-effect transistors were fabricated through the top-contact and bottom-gate geometry, with a $p^{++}Si/SiO_2/BCB/PCBM/ETL/Ag$ structure. Heavily doped p-type silicon <100> substrates with a 300 nm thermal oxide layer were purchased from Montco Silicon Technologies INC. After cleaning the substrate, the oxide layer was passivated with a thin divinyltetramethyldisiloxane-bis(benzocyclobutene) (BCB) layer. Fullerene thin films were spin-coated from chloroform solution (5 mg/mL). Interdigitated source and drain electrodes (W=1000 μm, L= 20 μm) were defined by evaporating a thin Ag layer (50 nm) through a shadow mask from the resistively heated Mo boat at 10^{-7} Torr. OFET characterization was carried out in a N_2 – filled glovebox using an Agilent 4155B semiconductor parameter S6 analyzer. The field-effect mobility, μ_{FET} was calculated from the linear fit of $(I_{ds})_{1/2}$ vs V_{gs} in the saturation regime. The threshold voltage (V_t) was estimated as the x intercept of the linear section of the plot of $(I_{ds})_{1/2}$ vs V_{gs}. The estimated FET mobilities are 0.084 $cm^2V^{-1}s^{-1}$ (PCBM), 0.036 $cm^2V^{-1}s^{-1}$ (TPA-PCBM), 0.049 $cm^2V^{-1}s^{-1}$ (BrTPA-PCBM) and 0.019 $cm^2V^{-1}s^{-1}$ (CNTPA-PCBM), respectively.
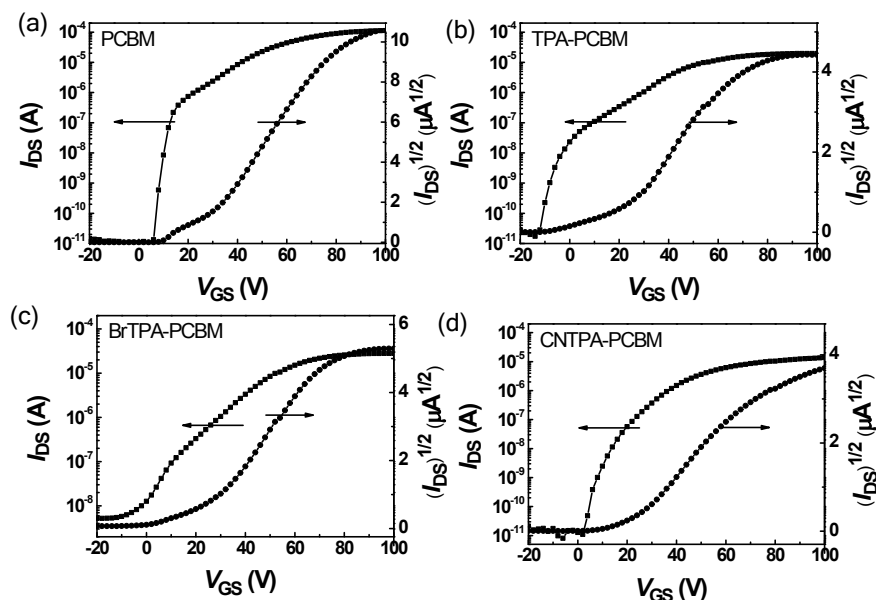

Figure S6. Transfer and output characteristics of n-FET for four fullerenes.

SCLC mobility measurements: Space charge limited currents have been tested in electron-

only devices with a configuration of ITO/ZnO/fullerene/Ca/Al. Fullerene thin films were spin-coated from its chloroform solution with fullerene film thickness ~ 55 nm. Assuming Ohmic injecting contacts and trap free transport at high voltages, the mobilities were determined by fitting the dark current to the model of a single carrier SCLC current with field dependent mobility, which is described as

$$J = \frac{9\varepsilon_r\varepsilon_0\mu_0 V^2}{8L^3}exp\left(\beta\frac{V}{L}\right)$$

Where J is the current, μ_0 is the zero-field mobility, ε_0 is the permittivity of free space, ε_r is the relative permittivity of the material, V is the effective voltage, and L is the thickness of the active layer. The estimated SCLC mobility in dark are 5.74×10^{-3} cm^{2}V^{-1}s^{-1} (PCBM), 7.90×10^{-4} cm^{2}V^{-1}s^{-1} (TPA-PCBM), 3.32×10^{-4} cm^{2}V^{-1}s^{-1} (BrTPA-PCBM) and 7.21×10^{-5} cm^{2}V^{-1}s^{-1} (CNTPA-PCBM), respectively.
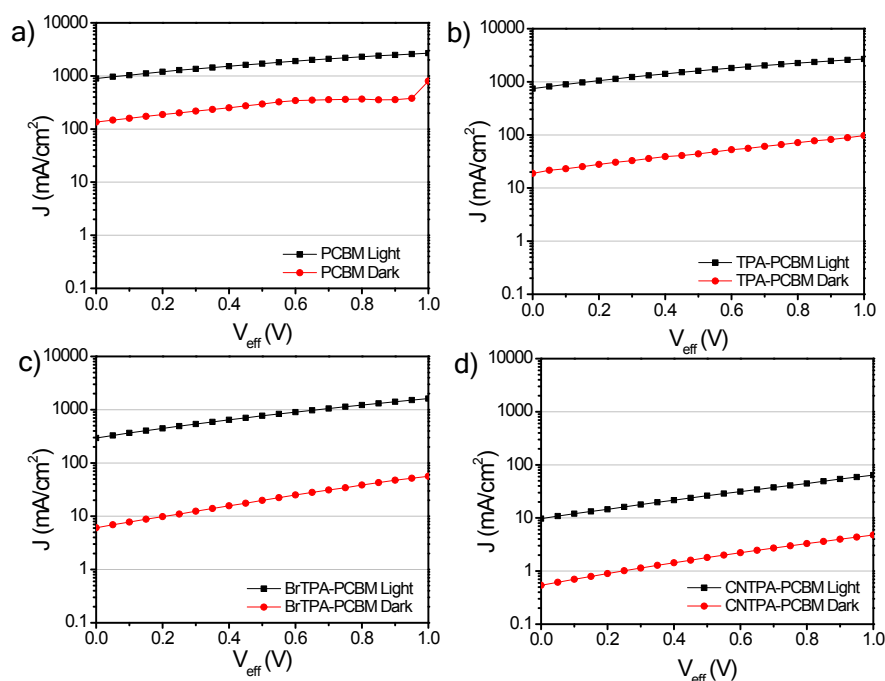
Figure S7. *J-V* characteristics under dark and light condition for devices consisting of different fullerene films. The effective voltage, V$_{eff}$ (*V*) is corrected for built-in voltage, V_{Bi}, arising from different in the work function of the contacts, and the voltage drop due to substrate series resistance (V_{RS}), such that = V_{APPL}-V_{RS}-V_{Bi}. (V_{APPL} is the applied voltage).
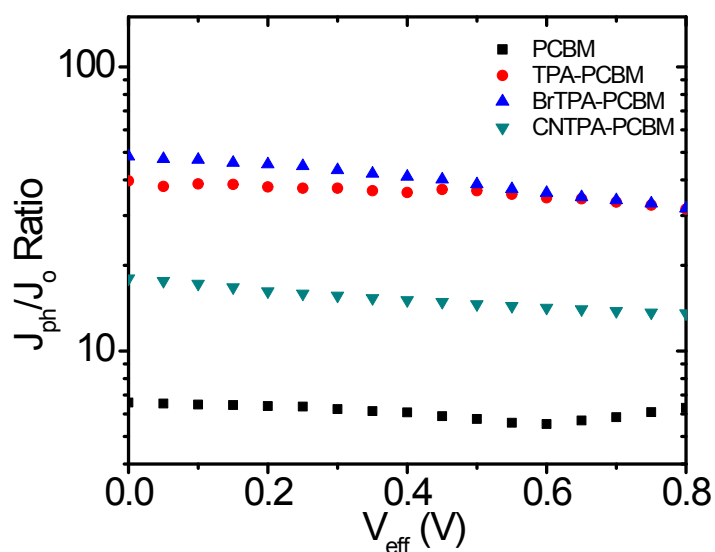
Figure S8. The plot of J_{ph}/J_o ratio against effective voltage, V_{eff}.

7. Reference

[1] Y. Zhang, H.-L. Yip, O. Acton, S. K. Hau, F. Huang, A. K. Y. Jen, *Chem.Mater.* **2009**, *21*, 2598.

[2] C.-Z. Li, S.-C. Chien, H.-L. Yip, C.-C. Chueh, F.-C. Chen, Y. Matsuo, E. Nakamura, A. K. Y. Jen, *Chem. Commun.* **2011**, *47*, 10082.

[3] Frisch, M. J.; Trucks, G. W.; Schlegel, H. B.; Scuseria, G. E.; Robb, M. A.; Cheeseman, J. R.; Scalmani, G.; Barone, V.; Mennucci, B.; Petersson, G. A.; et al. *Gaussian Development Version Revision H.13*, Gaussian Inc.: Wallingford, CT, 2010.

[4] Becke, A. D., Density-Functional Thermochemistry 3: The Role of Exact Exchange. *J. Chem. Phys.* **1993**, *98*, 5648-5652.

[5] Lee, C. T.; Yang, W. T.; Parr, R. G., Development of the Colle-Salvetti Correlation-Energy Formula into a Functional of the Electron-Density. *Phys. Rev. B.* **1988**, *37*, 785-789.

[6] Stephens, P. J.; Devlin, F. J.; Chabalowski, C. F.; Frisch, M. J., Ab-Initio Calculation of Vibrational Absorption and Circular-Dichroism Spectra using Density-Functional Force-Fields. *J. Phys. Chem.* **1994**, *98*, 11623-11627.